NATIONAL AERONAUTICS AND SPACE ADMINISTRATION

Technical Report 32-1146

Electrical Heater for Liquid Metals at Elevated Temperatures

L. Hays

D. O'Connor

G. Haskins

JET PROPULSION LABORATORY
CALIFORNIA INSTITUTE OF TECHNOLOGY
PASADENA, CALIFORNIA

August 15, 1967

Technical Report 32-1146

Electrical Heater for Liquid Metals at Elevated Temperatures

L. Hays

D. O'Connor

G. Haskins

Approved by:

D. R. Bartz, Manager
Research and Advanced Concepts Section

TECHNICAL REPORT 32-1146

Contents

Tables

Figures

Contents (contd)

Figures (contd)

Abstract

Design relations for high temperature electrical heaters of the conduction type for liquid metals are summarized in this report. The results of 500 hours testing of this type of heater in 2000°F lithium are given. The electrical resistivity and break-down strength of swaged beryllia and alumina were measured to 2200°F and these data are also presented. Design of a prototype heater for a 100-kWt cesium–lithium erosion loop is discussed, together with preliminary calculations for the heater for a 300-kWe liquid metal magnetohydrodynamic conversion system.

Electrical Heater for Liquid Metals
at Elevated Temperatures

I. Introduction

An investigation of the conceptual feasibility of a liquid metal magnetohydrodynamic (MHD) space power concept is currently being conducted at the Jet Propulsion Laboratory (Ref. 1). A future phase of this investigation is expected to include a 5-MW (thermal) system test using a cesium–lithium working fluid combination. A key component in this test, as in other high temperature liquid-metal systems, is the liquid-metal heater. In recent programs, heater failure has been a prominent operating difficulty encountered in experimental liquid-metal loops. A particularly stringent set of requirements exists for the MHD system heater. This heater must transfer 5 MW to lithium flowing at a maximum rate of 100 lb/s. Maximum temperature for the lithium may be as high as 2000°F in the eventual application, in which case the system would require refractory metal construction.

Direct-resistance heating of a liquid metal has been used quite successfully in recent high temperature investigations (Refs. 2, 3, 4). However, for large values of power, the use of expensive low-voltage, high-current power sources are required to avoid excessive heater size and fluid pressure loss. Because of the high currents in larger

installations, bus problems may be encountered. Also, direct current power is desirable to avoid skin effect and fatigue due to fluctuating magnetic force fields.

Radiant heating has also proved successful for high temperature applications (Ref. 5). This method allows the use of medium-voltage power sources and moderate current levels. However, for large inputs of power the required heat transfer area may become excessive in size and necessitate fabrication of large, complex refractory metal structures.

The third type of heating—which was selected for use—is that of the conduction heater. Heat is generated in the current element and transferred by conduction across an electrical insulator and metal sheath to the liquid-metal stream. The electrical insulation is usually provided by swaging the sheath onto ceramic material. Conduction heaters have been used extensively for liquid-metal heating (Refs. 6, 7, 8), but at lower power and temperature levels than those required by the liquid MHD system tests. This type of heater enables the use of medium voltage, and moderate current power sources; and results in a compact component. However, the attainable level of reliability is not known for higher temperatures.

The three most important failure modes for conduction heaters at elevated temperatures are thought to be electrical breakdown of the insulator, degradation of the ceramic in the region of sheath weldments, and local overheating in the region of center-conductor attachment to the bus. The method of obviating these problems has been to use a simple configuration which is amenable to analysis, and to select materials and fabrication methods which are compatible at the predicted temperatures. The sequence adopted for development of the 5-MW heater comprises four phases:

(1) Analysis and preliminary sizing of the 5-MW heater that is based on existing high-temperature electrical-breakdown data for fired ceramics.

(2) Testing of geometrically similar heater elements in lithium at elevated temperatures to determine breakdown strength and insulator leakage currents for swaged ceramics, and to verify design and fabrication methods.

(3) Operation of a geometrically similar heater in a 100-kW cesium–lithium erosion loop to determine reliability and verify design.

(4) Final design of the 5-MW heater, incorporating test data from (2) and (3).

This paper presents the results of the first and second phases, and discusses fabrication details of the 100-kW lithium heater for the third phase.

II. Heater Design

The starting point in the heater design was to examine the relationship between center-conductor temperature, heater dimensions, and electrical characteristics as a function of the allowable insulator field strength and material properties.

In this analysis the leakage currents, axial temperature variation, and contact resistances were neglected. Consider the configuration in Fig. 1. If a total of N heating elements is used with n elements connected in series, the total power is given by Ohm's law as

$$P_e = \frac{23.9 V^2 N d_c^2}{\rho n^2 L} \tag{1}$$

where the quantities and units are defined in Nomenclature.
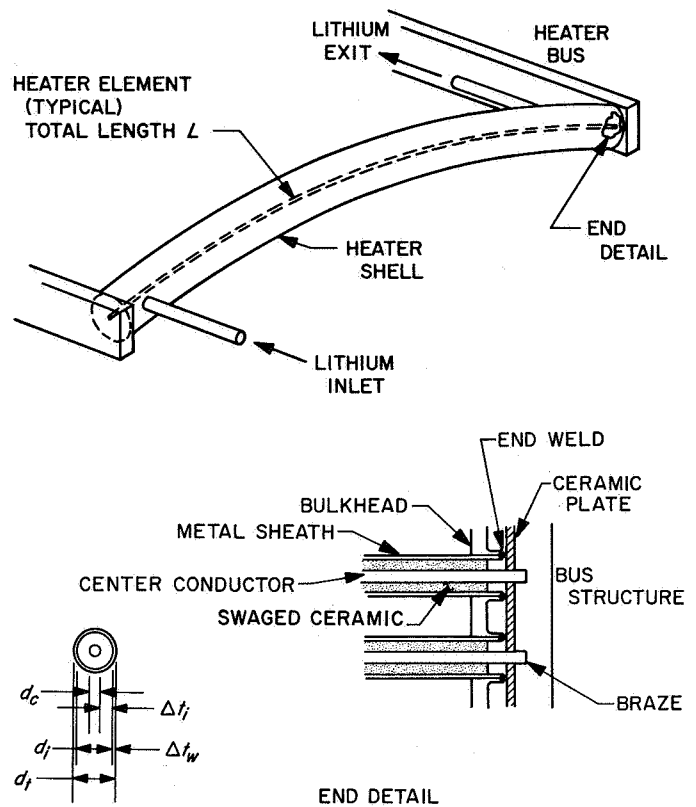
Fig. 1. Schematic of conduction heater configuration and nomenclature

The temperature difference from sheath to center is obtained by considering conduction through concentric cylinders. The surface heat flux is expressed in terms of the heater dimensions to give the temperature difference

$$\theta_c = \frac{0.543 P_e}{NL} \left[\frac{\ln (d_i/d_c)}{k_i} + \frac{\ln (d_t/d_i)}{k_t} \right] \tag{2}$$

If the design field strength on the ceramic is E, then the minimum insulator thickness which can be used is simply

$$\Delta t_i \approx \frac{V}{E} \tag{3}$$

and (2) becomes

$$\theta_c = \frac{0.543 P_e}{NL} \left[\frac{1}{k_i} \ln \left(1 + \frac{9.8 V^2 N^{1/2}}{nE P_e^{1/2} \rho^{1/2} L^{1/2}} \right) \right.$$
$$\left. + \frac{1}{k_t} \ln \left(1 + \frac{\Delta t_w}{\frac{0.102 n P_e^{1/2} \rho^{1/2} L^{1/2}}{V N^{1/2}} + \frac{V}{E}} \right) \right] \tag{4}$$

This expression can be used for a specified power output P_e, and power source voltage V, to determine the influence of element length L, total number N, and series connection number n, on the sheath–center-conductor temperature difference, θ_c, and the center-conductor diameter, d_c.

For example, Figs. 2 and 3 were calculated for an output power, P_e, of 5000 kW; a voltage, V, of 150 V; and an allowable gradient, E, of 3 V/mil. The value of 3 V/mil for the ceramic insulator was based on a measured breakdown strength of 4 V/mil reported in Ref. 9 for alumina and magnesia at 1200°C (2190°F) and beryllia at 1000°C. Beryllia was chosen as the insulator for these calculations because of its compatibility with refractory metals at elevated temperatures and its high thermal conductivity. The sheath was Cb-1Zr, with a wall thickness of 0.030 in., and was chosen for its compatibility with lithium and its adaptability to fabrication methods. The center conductor was tantalum, chosen for its high resistivity, and ductility in the recrystallized condition. Properties were evaluated at average temperatures, while assuming a design temperature of 2000°F for the sheath and a design temperature of 2400°F for the center conductor.

As shown in Fig. 2, increasing the number of heating elements results in lower centerline temperatures and smaller center-conductor diameters. Lower centerline temperatures are also produced as more elements are operated in series, but for this case the diameter increases with increasing values of n. For example, 40 elements
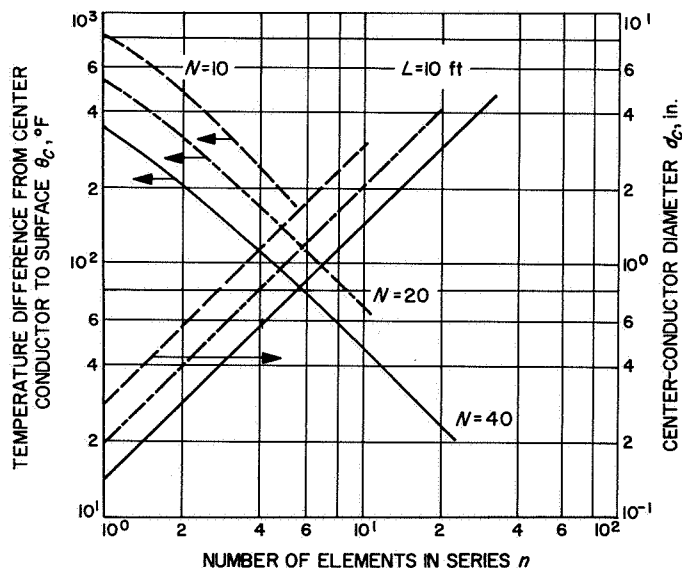
Fig. 2. Temperature difference and center-conductor diameter vs number of heating elements connected in series
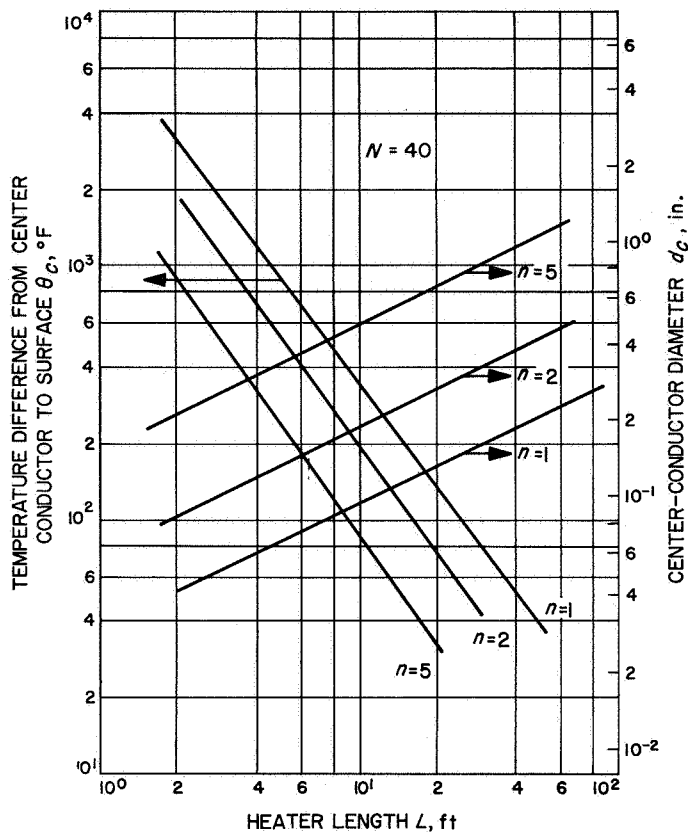
Fig. 3. Temperature difference and center-conductor diameter vs heater length for 40 heating elements

operating in groups of 2 in series instead of all in parallel lowers the centerline temperature difference from 350 to 200°F. For parallel operation, a decrease in the number of elements from 40 to 10 would increase the centerline temperature difference from 350 to 800°F, which would exceed the design value.

The influence of varying element length is shown in Fig. 3. For 40 elements operating in parallel, a change in element length from 10 to 5 ft would increase the centerline temperature difference from 350 to 900°F. A decrease of this length would require a decrease in center-conductor diameter from about 0.15 to 0.10 in. to satisfy the voltage and power requirements.

Based on these calculations, a reasonable heater design which should satisfy reliability considerations by having a moderate centerline temperature would be composed of 40 parallel elements ($n = 1$) 10 ft in length. This would produce a centerline temperature difference of about 350°F with a conductor diameter of 0.16 in. The sheath or outer diameter would be 0.32 in. and the insulator thickness, 0.050 in.

An arrangement of these heaters in a square array with $s/d = 2$ would result in a heater shell with an inside diameter of 4.5 in. and a length of 10 ft for the 5-MW unit. Application of liquid-metal heat-transfer relations for in-line rod bundles (Ref. 10) yields a temperature drop of about 20°F from the sheath wall to the coolant bulk temperature for 100-lb/s lithium flow at about 1975°F average bulk temperature and the required heat-transfer rate. For a maximum lithium temperature of 2000°F this would result in a centerline temperature of about 2400°F, which is certainly consistent with the assumptions of the analysis and compatible with available materials and fabrication techniques.

Thermally induced stresses in conduction heaters of this type for these values of temperature difference appear to be moderate if a curved configuration is used. A summary of thermal stress calculations for the 100-kW heater for the cesium–lithium erosion loop is given in Appendix B. For this specific heater configuration a bow of 3 in. for the total length of 30 in. gave end loadings of less than 0.6 lb on each of the four heating elements. The estimated centerline to lithium temperature difference of 100°F was doubled and applied to the entire heating element for this calculation to yield a very conservative result. With less conservative assumptions, a bow of about 1 ft over the 10-ft length of the 5-MW heater should result in acceptable end loadings. For such larger heaters, other means (such as a bellows) for accommodating differential expansion between the case and heating elements might be used instead of a curved configuration.

The moderate current levels ($\sim$ 30,000 A) enable radiantly cooled buses, with their attendant simplicity and reliability, to be used to supply power to the heater. The method of attaching the sheaths to the heater shell is to recess the ceramics, to weld, and then to braze the space behind the weld with zirconium (see Fig. 1). The reason for recessing the ceramic is to avoid overheating when the weldments are performed. The exposed center conductor (see Fig. 1) will generate a significant amount of heat which must be removed and dissipated by the bus to avoid excessive temperature in this region. In the following discussions, the recessed length, L_1, is the length from the bus to the beginning of the ceramic (see Fig. 4). In order to determine the influence of the recessed length on the minimum bus length, L_2, a simplified analysis was performed to guide the heater designs tested. The following assumptions were made for the analysis:

(1) The exposed conductor is insulated in the radial direction.

(2) The maximum temperature allowable is the centerline heater temperature (2400°F in the previous example).

(3) The heat flow is one-dimensional.

With these assumptions, the bus dimensions can be determined. For example, for the cylindrical conductor illustrated by Fig. 4:

$$T_b = T_c - \frac{q''' L_1^2}{2k_1} \tag{5}$$

where

$$q''' = \text{volumetric heat release} = 0.181 \frac{I^2 \rho}{d_1^4} \tag{6}$$

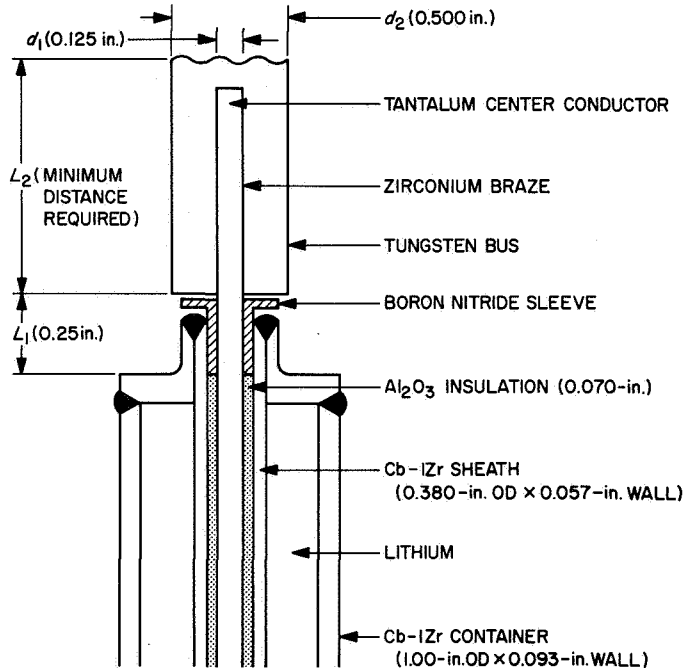**Fig. 4. End detail of lithium heater**

The heat transferred by radiation from a cylindrical bus heated at one end to an infinite sink at a much lower temperature is

$$Q_r = \sigma \varepsilon \, \eta_f \pi \, d_2 L_2 T_b^4 \tag{7}$$

(neglecting the bus I^2R heating since it is small compared with the end heating) where

$$\eta_f = f\left(\frac{2\sigma\varepsilon \, T_b^3 L_2^2}{k_2 d_2}\right) \tag{8}$$

The relation between η_f and *radiation modulus* for a cylindrical fin is given in Fig. 5 (from Ref. 11).
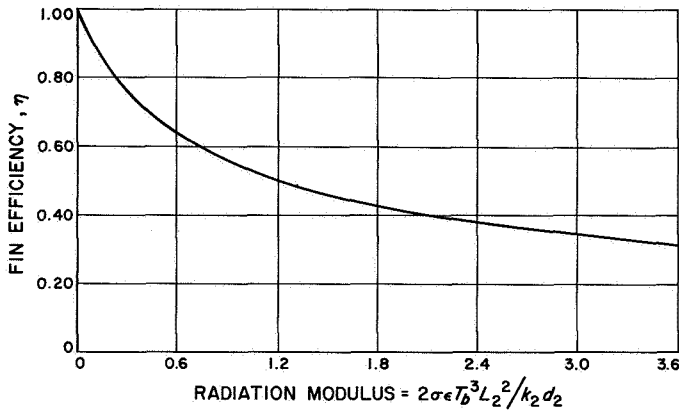

Fig. 5. Fin efficiency vs radiation modulus for a cylindrical conductor

Now to find the value of bus length L_2, which will reject the required heat, solve for L_2 using (5) and (7):

$$L_2 = 0.0454 \frac{I^2 \rho L_1}{\sigma \varepsilon \, \eta_f \, d_1^2 \, d_2 \, T_b^4} \qquad (9)$$

Equation (9) can be solved by trial and error (using Fig. 5) for the value of L_2 which will reject the required heat. Figure 6 presents the results of such a calculation for one of the test heaters. The bus length L_2, required to maintain the exposed conductor temperature at a value less than the centerline temperature T_c, is plotted as a function of the exposed conductor length. The particular values of I, d, and T_c were 400 A, 0.150 in., and 2370°F. The influence of different bus diameters is also shown. As can be seen, beyond a recess of about ⅛ to ¼ in. the required bus length increases rapidly. For these parameters, no solution exists to the equations beyond a recess of about ⅜ in., indicating that radiant cooling could not be used without increasing the bus diameter, emissivity, or maximum allowable temperature. The recessed distance of the initial test design was ¼ in. From the curve, for a bus diameter of ½ in., a minimum bus length of about 1½ in. is required to dissipate the heat. Hence, any bus length in excess of this value would clearly be acceptable. Further increases in L_2 will simply lower the maximum temperature of the exposed center conductor.

Similar calculations can be performed for a planar bus with multiple conductors by assigning an area to each conductor and applying the appropriate geometric relations for radiant transfer.
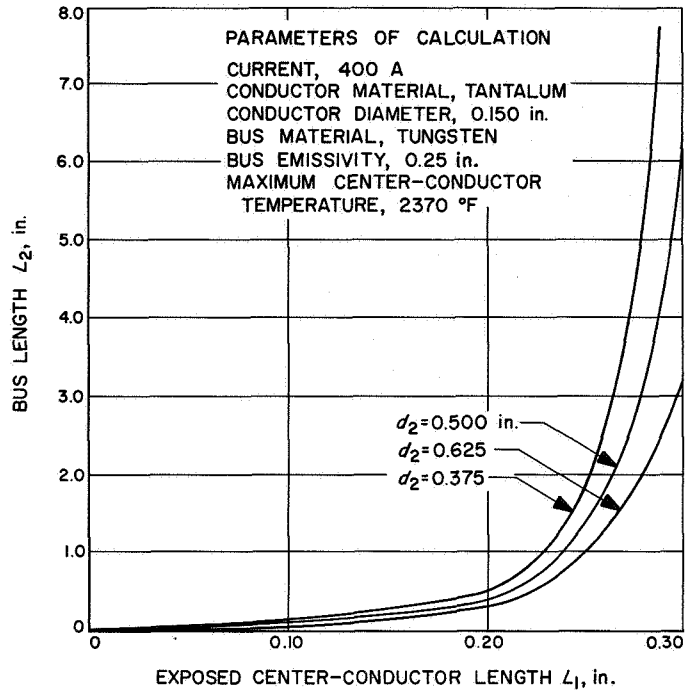
Fig. 6. Minimum bus length required for radiant cooling of exposed center conductor in a test design

III. Test Heater Configurations and Experimental Arrangement

Three test heaters were fabricated with radiantly cooled buses in order to demonstrate the validity of the design and to measure the high temperature electrical properties of the swaged ceramic insulation. The first of these heaters was welded into a test section which was subsequently filled with lithium for high temperature operation. The others were operated without lithium, rejecting the generated heat by radiant transfer. Table 1 gives a summary of the design parameters and materials of construction for the three heaters.

The initial test heater which operated in lithium had a configuration with a tantalum center conductor of 0.125 in. in diameter, 0.070 in. of swaged alumina insulation, and a Cb-1Zr sheath with a diameter of 0.380 in. The swaging process for this unit was performed by a commercial firm to specifications of the Jet Propulsion Laboratory (JPL). This design is shown schematically in Figs. 7 and 8 as it was installed in a lithium container with expansion chamber. Tungsten–5% rhenium versus tungsten–26% rhenium thermocouples were attached to the surface by spot-welding, but the primary temperature measurement was made with an optical pyrometer reading of the surface temperature.

Table 1. Dimensions of experimental heaters

Heaters	Dimensions					
	d_c, in.	Δt_i, in.	d_t, in.	L, in.	d_2, in.	L_2, in.
Alumina-Lithium heater	0.125	0.070	0.380	12	0.50	3.00
Beryllia radiant heater	0.157	0.045	0.300	13.25	0.50	3.00
Alumina radiant heater	0.157	0.045	0.300	13.25	0.50	3.00
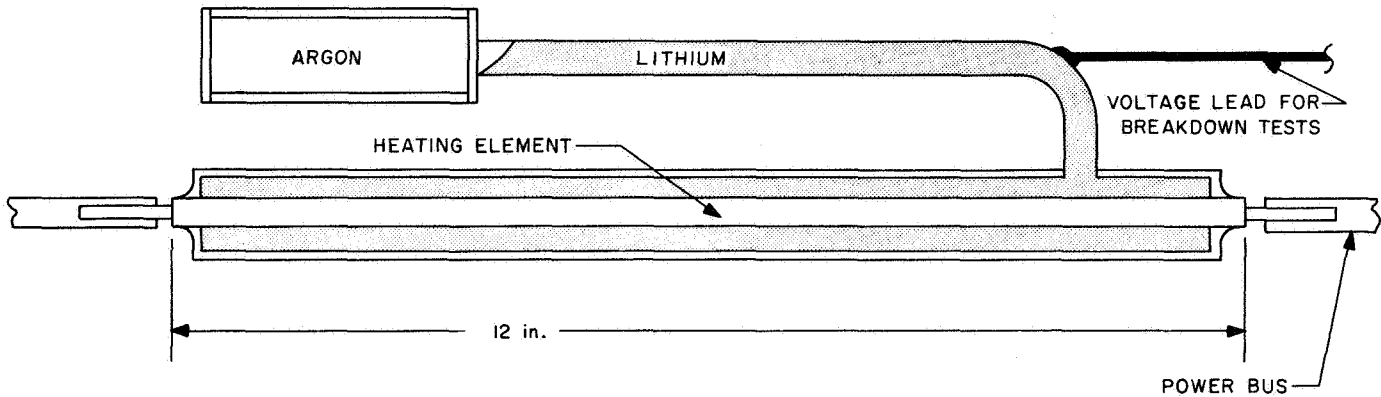
Fig. 7. Schematic of heater test design
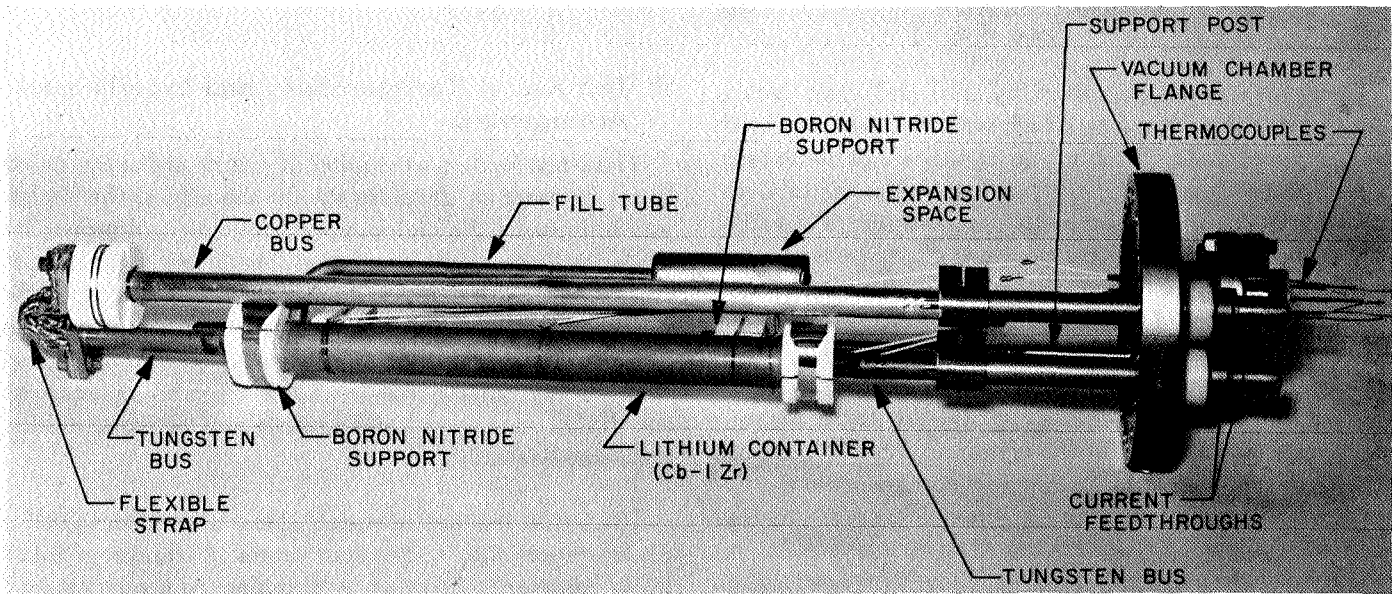
Fig. 8. Lithium heater experiment, showing flange mounting

The ceramic was recessed by ¼ in. in this initial design to insure good heater weldments. Welding and zirconium brazing were performed in an inert gas dry box (Ref. 12) and the unit was subsequently annealed at 2200°F for one hour in a vacuum furnace. Boron nitride spacers and supports were used which provided an increased path for heat flow from the exposed conductor.

After the container was filled with lithium from a filtered stainless steel loading system, the basic heater capsule was mounted on the end flange of an ion-pumped, water-cooled, vacuum chamber as shown in Fig. 8. During operation in the chamber, the heat generated in the heater was conducted through the lithium and container wall and transferred to the outside wall of the vacuum cham-
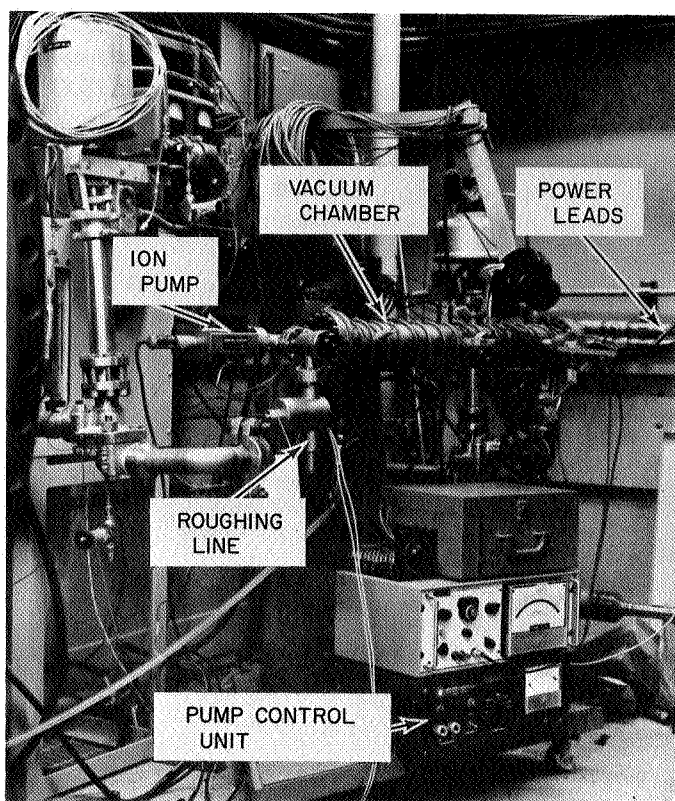
Fig. 9. Lithium heater experimental apparatus

ber by radiation. The wall of the Cb-1Zr test section was grit-blasted to enhance the emissivity.

A silicon-rectifier dc-power supply was used to supply the heater current through brazed vacuum feedthroughs. Several small dc-power supplies were connected in parallel to apply voltage to the heater sheath for determining ceramic resistivity and breakdown. Fig. 9 shows the final test setup with the heater at temperature.

The second heater tested had beryllia insulation swaged between the tantalum center conductor and Cb-1Zr sheath. The diametral dimensions of this heater (see Table 1) and the third one tested were identical with the prototype unit to be operated in a cesium–lithium erosion loop. The beryllia heater was tested in the same vacuum chamber as the lithium heater, except with diffusion pumping instead of ion pumping. Similar mounting arrangements were used. The third heater, which had alumina insulation, was tested in an identical vacuum chamber with diffusion pumping.

Figure 10 is a photograph of the test setup for the second and third units. Figure 11 shows the beryllia radiant heater in test operation at 2100°F.
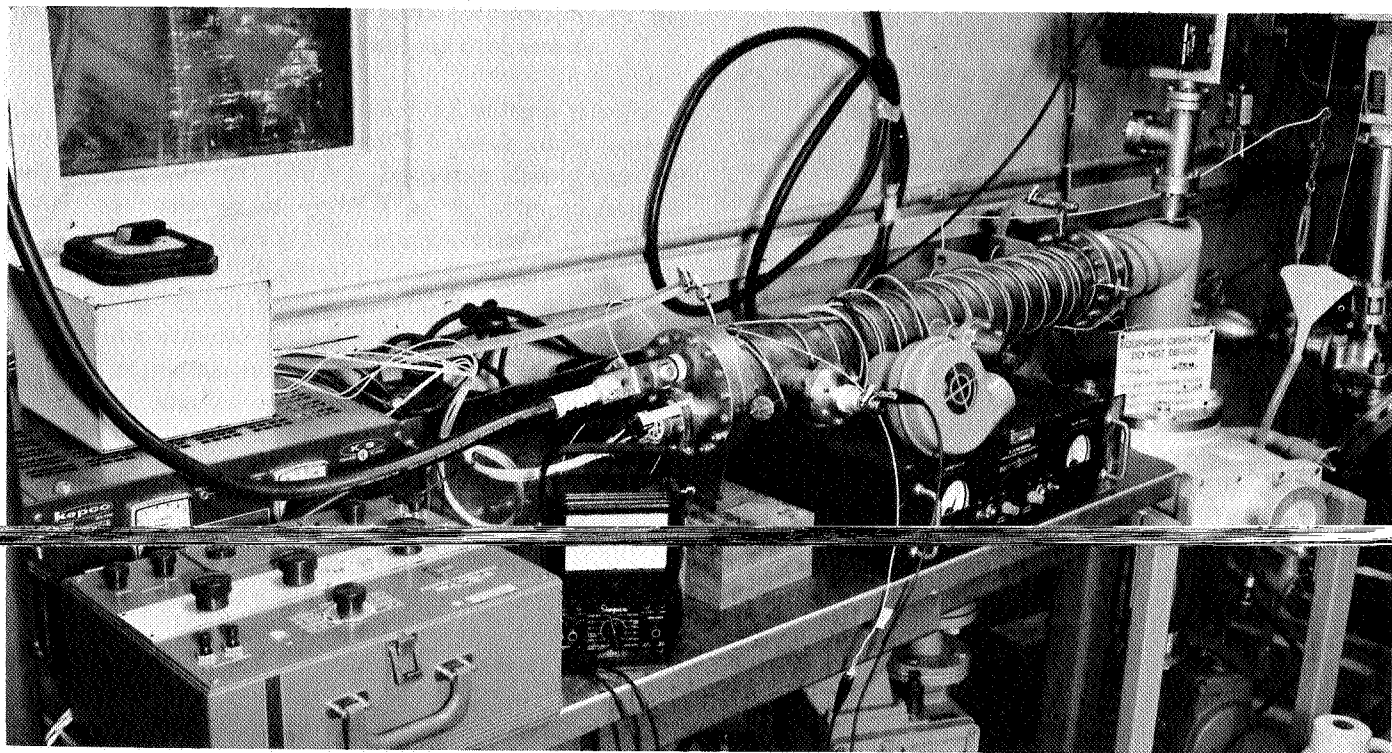
Fig. 10. Radiant heater experimental apparatus
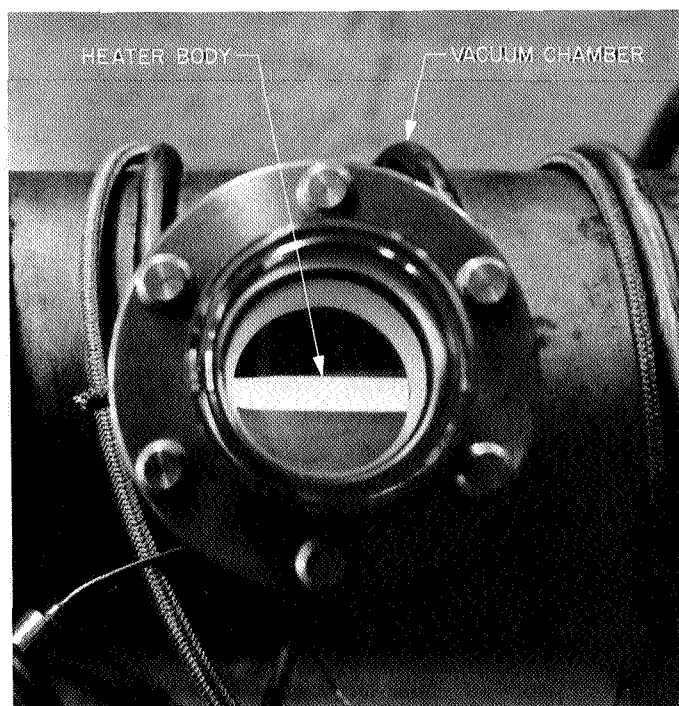
Fig. 11. Beryllia radiant heater at 2100°F

IV. Initial Test Results

A. Lithium Heater

After the outgassing, the lithium heater was operated continuously for 500 h, maintaining a bulk lithium temperature of approximately 2080°F. This is a corrected pyrometer temperature reading based on a spectral emissivity of 0.4. (The uncorrected reading was 1940°F.) During the course of the test, the temperature varied between 2000 and 2100°F because of drift in the power supply, but at no time was it less than 2000°F. As shown in Fig. 12, approximately 2 kW were required to maintain the heater at its peak temperature. The heat flux during this
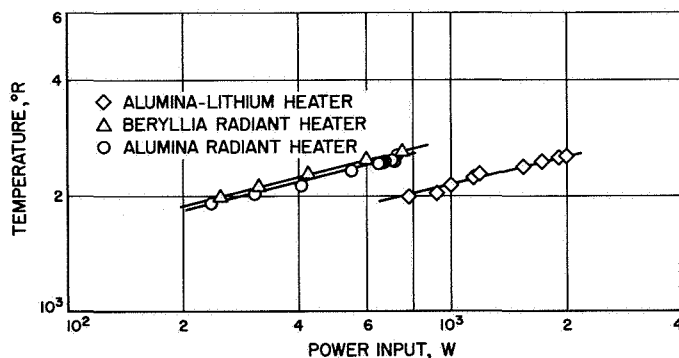
Fig. 12. Surface temperature vs input power

test was 130 W/in.^{2} at the heater surface. The center-conductor temperature was between 2360°F (calculated from the surface temperature and heat flux) and 2540°F (estimated from the measured increase in resistance of the tantalum). The low bus temperatures measured ($\approx 500°F$) qualitatively confirmed the radiant cooling calculations discussed under *Heater Design*.

After the 500-h run, a dc potential was applied to the sheath to determine the resistivity of the alumina in the swaged condition and the maximum field strength it could support. These data are given in Appendix A. Figure 13 presents the results of these tests.
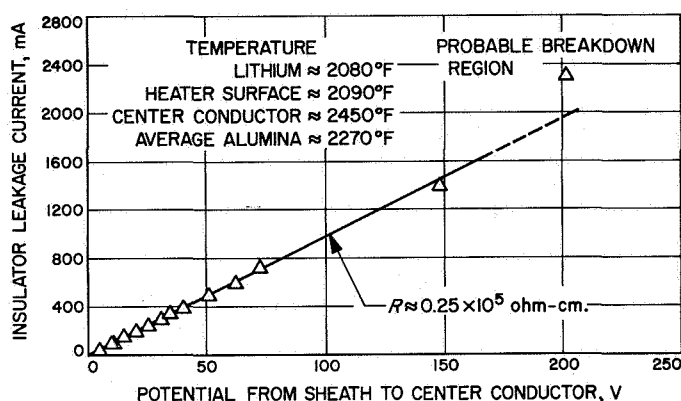
Fig. 13. Alumina insulator leakage current for the lithium heater as a function of applied potential

A linear relation between leakage current and potential existed up to about 3 V/mil. The average resistivity for this region was measured at 0.25×10^5 ohm-cm for the swaged alumina at an average temperature of about 2270°F. This can be compared to a value of 1×10^5 ohm-cm reported in the literature for fired alumina at this temperature (Ref. 9). Above an applied voltage of 3 V/mil, the leakage current showed a sharp increase which may have been due to the beginning of breakdown in the ceramic as discussed later. The heater current had to be decreased as the leakage current increased, to maintain a constant ceramic temperature. This decrease in resistivity may, therefore, have been due to local temperature increases which resulted from the difficulty in coordinating these two currents. In any case, the tests demonstrated the basic feasibility of using swaged conduction heaters at elevated temperatures with field strengths up to 3 V/mil across the ceramic.

Examination of the heater after the test revealed slight reactions between the alumina and tantalum, and between the boron nitride and Cb-1Zr in the region of the

end weldment. These reactions are known and were expected but are not serious at the temperatures of interest. No similar reaction occurred between the beryllia and tantalum at the temperatures of interest. No lithium penetration occurred in the weld regions, and the end weldments appeared mechanically sound after test.

B. Radiantly Cooled Test Heaters

The relation between surface temperature and heater power for the beryllia and alumina radiant heaters is shown on Fig. 12. The curves are approximately the same for these two units because of their similar configurations. Only about 650 W were required for these heaters to reach 2000°F as compared with 2000 W for the lithium heater. Thus, the surface heat flux at 2000°F was about 40–50 W/in.², which is about one-third the value reached during the lithium test.

The prime objective of these tests was to measure the resistivity of swaged alumina and beryllia as a function of temperature. The results are summarized in Fig. 14 and Appendix A. The beryllia exhibited higher resistivity than the alumina over the entire temperature range tested. At 2200°F, for example, the resistivity of the beryllia was 10^5 ohm-cm, while that of the alumina was only 3.5×10^4. The applied dc potential across the beryllia insulation varied from 50 to 200 V, with no breakdown. This corresponds to a maximum field strength of 4.4 V/mil on the beryllia (at a temperature of 2100°F). With this alumina heater, the maximum potential applied was 150 V. This field strength (3.3 V/mil) produced breakdown of the ceramic after a few hours operation at 2100°F. Thus, in this application beryllia appears to be a much more suitable insulator than alumina.

Resistivity data for fired beryllia and alumina and for beryllia powder are shown on this plot for comparative purposes. The swaged beryllia data fall between the values for compressed powder and fired ceramic, but are closer to the latter. For example, at 2200°F Bacon's curve for fired beryllium oxide (Ref. 13) gives a value of 7.4×10^4 ohm-cm versus about 1×10^5 ohm-cm for the experimental curve for swaged beryllia. Ryshkewitch (Ref. 14) gives a value of 3.5×10^6 ohm-cm at this temperature for compressed beryllium oxide powder. The data for the swaged alumina fall somewhat below the values given by Knoll (Ref. 15) for fired alumina. At 2100°F the measured value for swaged alumina was about 7×10^4 ohm-cm versus about 2×10^5 ohm-cm for the fired material.

The influence of the time at elevated temperature on resistivity was investigated for the beryllia heater. Figure
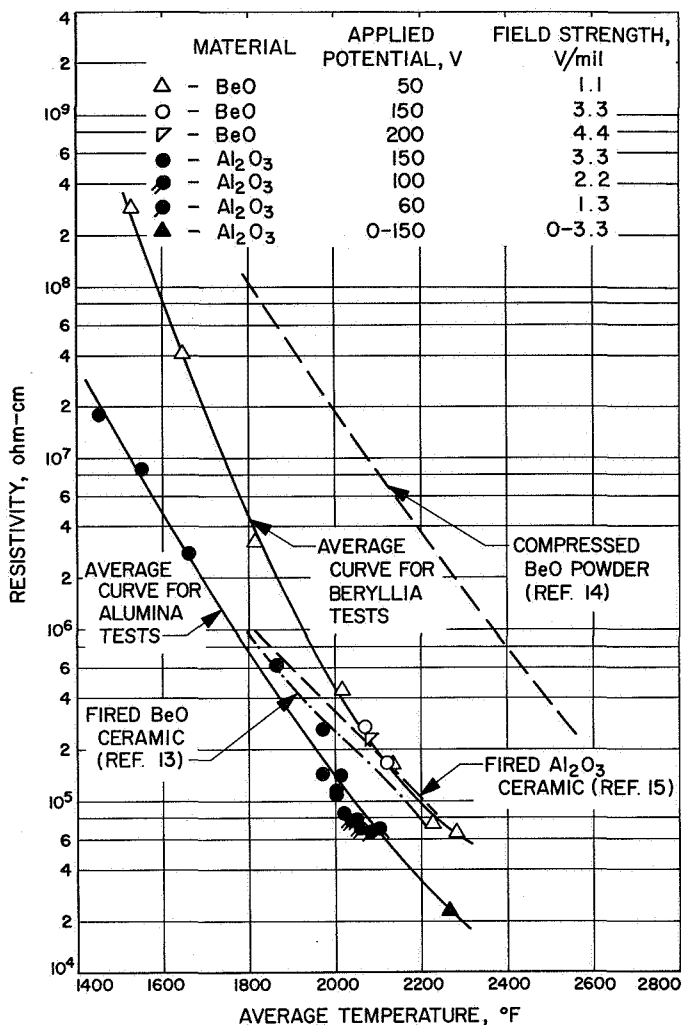
Fig. 14. Resistivity for swaged ceramics as a function of temperature

15 summarizes the results of resistivity measurements versus the duration of time at temperatures above 2000°F. The ordinate is the ratio of the log of the measured resistivity to the log of the initial resistivity. The temperatures
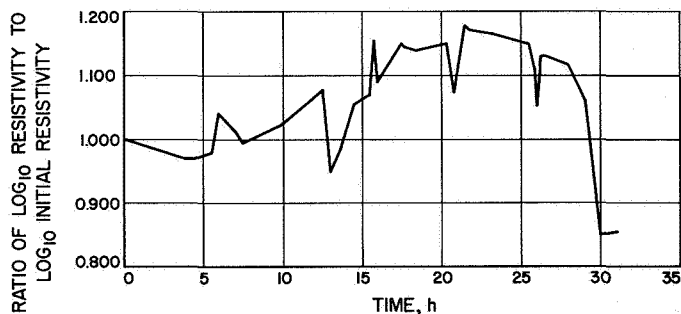
Fig. 15. Change in resistivity vs time for beryllia at 1990–2260°F
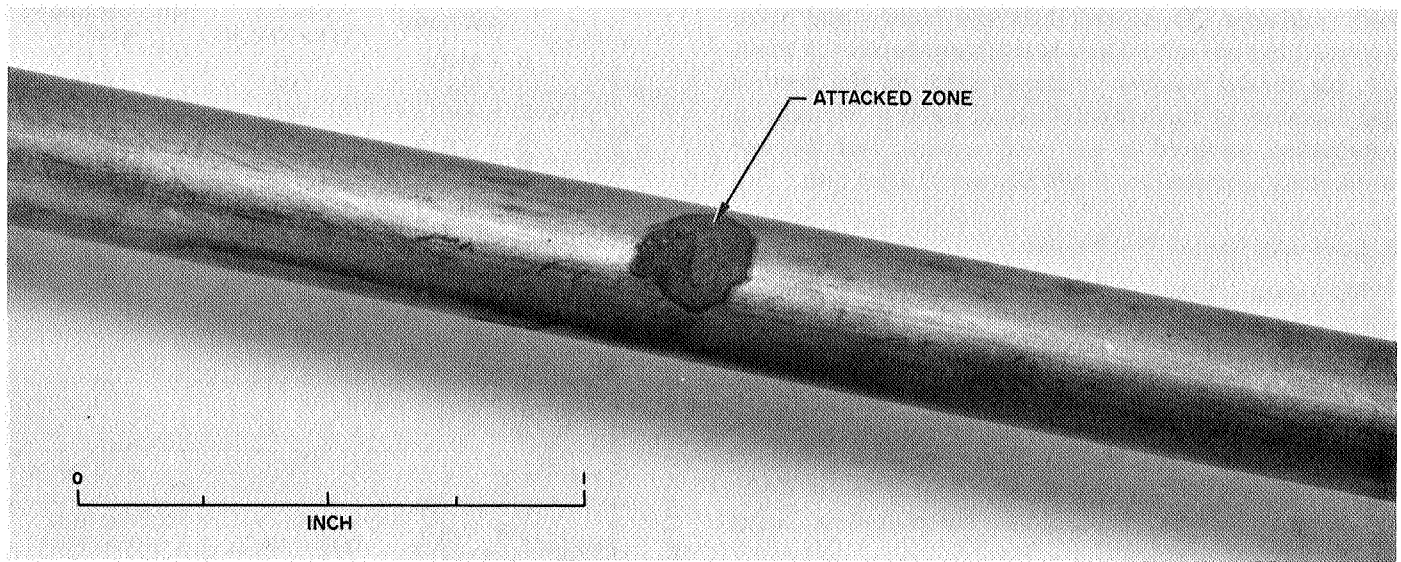
Fig. 16. Reaction zone on radiant beryllia heater
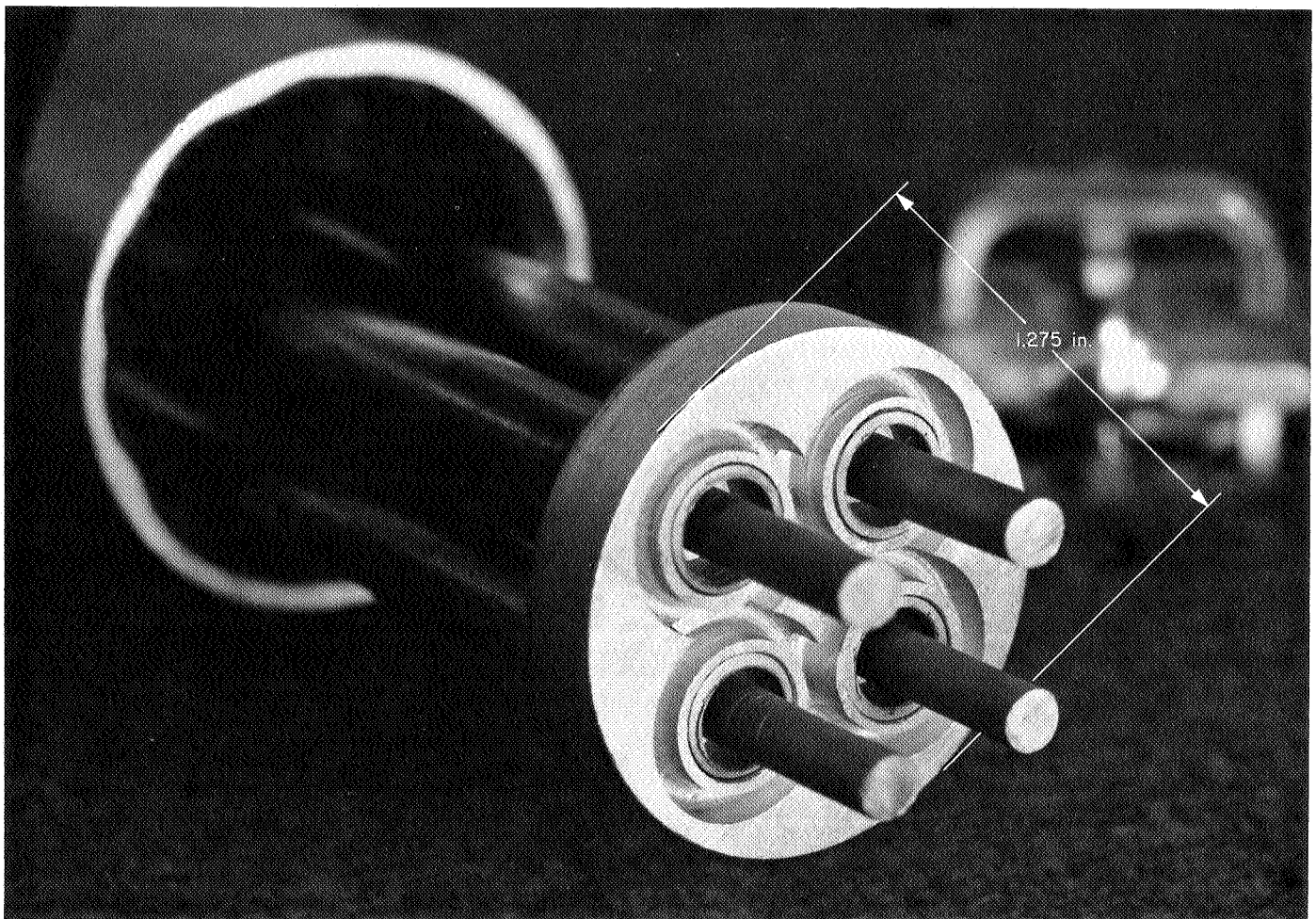
Fig. 17. End detail of 100-kWt heater before welding

during this test varied from 2000 to 2260°F so the values for initial resistivity correspond to those of Fig. 14. As can be seen, the resistivity underwent an erratic overall increase during the initial 20 h. After that time it declined gradually, until at 27 h when it decreased sharply. The test was discontinued after 31 h to see if the cause of the decrease could be found. During the examination, a spot on the sheath was discovered where the columbium had been attacked either by impurities in the vacuum atmosphere or in the beryllia insulation. This damage is shown in Fig. 16.

The inherent ruggedness of this type of heater was demonstrated by 20 thermal cycles from ambient to 2000°F on the beryllia unit and greater than 100 cycles from 350 to 2000°F on the alumina unit. For the latter tests the total time of the heat–cool cycle was 15 min, with a heating rate of greater than 300°F/min.

Tests in a flowing lithium system are planned for the near future. The heater for this cesium–lithium erosion loop (Ref. 1) is shown prior to welding, in Figs. 17 and 18. It consists of four heating elements, 2½ ft long, in a Cb-1Zr shell. The heating elements have tantalum center conductors with swaged beryllia insulation and Cb-1Zr sheaths. The ceramic is recessed by ⅛ in. for welding. The design conditions on this heater are 300 W/in.^{2}, with the resulting temperature difference from center conductor to sheath of about 100°F. A stress analysis on the heater indicated a need for a curved configuration to relieve thermal expansion stresses. This analysis is summarized in Appendix B.

Operation of this heater should result in sufficient data for final design of a 5-MW lithium heater. A satisfactory degree of reliability, a compact design, and an inexpensive system appear to be attainable with the conduction type of heater.

Fig. 18. 100-kWt heater assembly before welding

Appendix A

Summary of Test Data

Table A-1. Data on three heaters

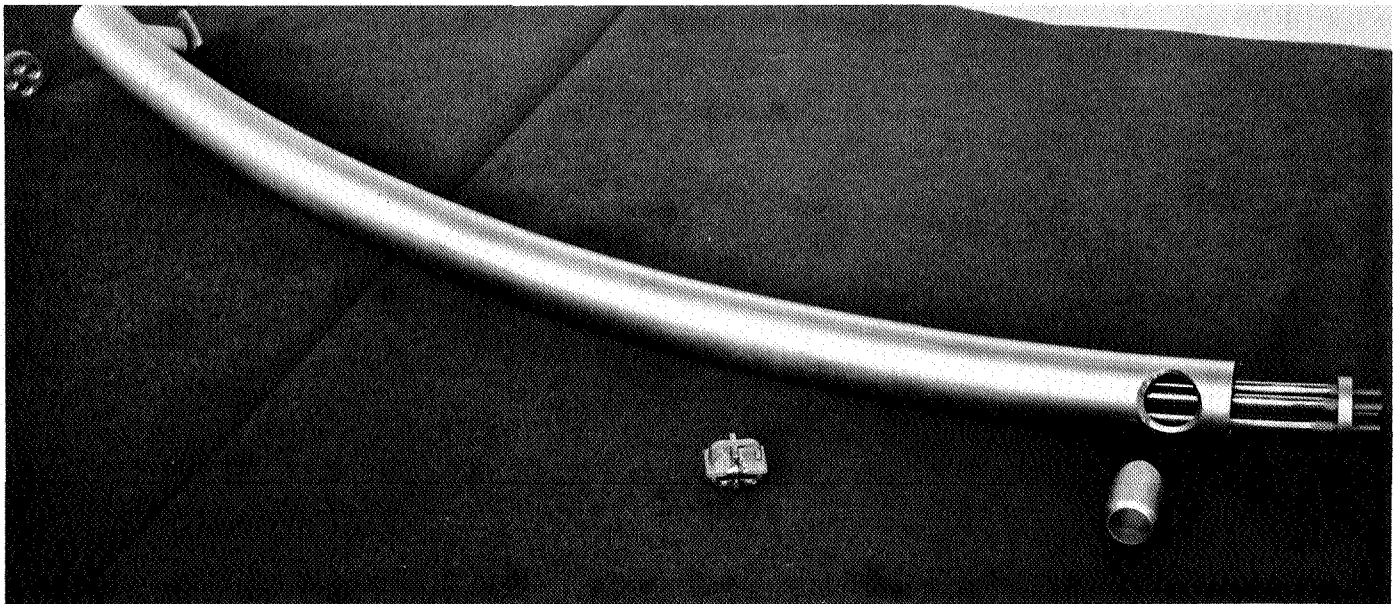| Run no.	Temperature, °F	Heater voltage, V	Heater current, A	Heater power, W	Sheath voltage, V	Sheath current, mA	Ceramic resistance, ohm	Ceramic resistivity, ohm-cm
			1. Alumina-lithium heater					
	Surface, Li container							
1	1524	3.90	200	780	—	—	—	—
2	1604	4.38	210	920	—	—	—	—
3	1686	4.78	210	1005	—	—	—	—
4	1769	—	—	1150	—	—	—	—
5	1811	—	—	1190	—	—	—	—
6	1921	—	—	1550	—	—	—	—
7	1991	—	—	1730	—	—	—	—
8	2040	—	—	1907	—	—	—	—
9	2064	7.24	275	1995	—	—	—	—
	Ceramic, average (est.)							
10	2270	7.24	275	1995	4.6	50	92	2.4×10^4
11					9.9	100	99	2.59×10^4
12					15.1	150	100	2.62×10^4
13					20.4	200	102	2.68×10^4
14					25.4	250	101	2.65×10^4
15					30.4	300	101	2.65×10^4
16					34.8	350	100	2.62×10^4
17					40.4	400	101	2.65×10^4
18					10.4	100	104	2.72×10^4
19					51.4	500	107	2.80×10^4
20					62.5	600	104	2.72×10^4
21					72.4	730	99.2	2.60×10^4
22					148.4	1400	106	2.78×10^4
23					196.4	2300	85.4	2.24×10^4
			2. Beryllia radiant heater					
1	1526	1.67	150	251	50	0.07	7.2×10^5	2.9×10^8
2	1644	1.98	160	317	50	0.50	1.0×10^5	4.08×10^7
3	1810	2.35	180	423	50	6.33	7.9×10^3	3.22×10^6
4	2016	3.00	200	600	50	44	1.07×10^3	4.38×10^5
5	2131	3.38	220	744	145	450	4.00×10^2	1.63×10^5
6	2065	3.20	—	—	150	265	6.65×10^2	2.71×10^5
7	2115	3.60	—	—	150	370	4.05×10^2	1.65×10^5
8	2079	3.30	—	—	200	352	5.70×10^2	2.32×10^5
9	2223	4.0	—	—	50	280	1.78×10^2	7.28×10^4
10	2277	4.2	—	—	50	310	1.60×10^2	6.53×10^4

Table A-1 (contd)

Run no.	Temperature, °F	Heater voltage, V	Heater current, A	Heater power, W	Sheath voltage, V	Sheath current, mA	Ceramic resistance, ohm	Ceramic resistivity, ohm-cm
				3. Alumina radiant heater				
1	1453	1.92	123.5	237	150	3	4.4×10^4	1.80×10^7
2	1549	2.15	143.0	307	150	7	2.1×10^4	8.62×10^6
3	1658	2.80	146.2	409	150	22	6.8×10^3	2.78×10^6
4	1865	3.20	172.4	550	150	98	1.52×10^3	6.24×10^5
5	1978	3.60	183.1	659	150	230	6.50×10^2	2.67×10^5
6	2010	3.75	187.6	704	150	440	3.40×10^2	1.39×10^5
7	2000	3.65	185.7	676	150	500	2.80×10^2	1.15×10^5
8	2010	3.65	186.1	679	150	600	2.50×10^2	1.03×10^5
9	2018	3.75	187.4	703	100	490	2.05×10^2	8.42×10^4
10	2005	3.65	185.7	676	150	90	2.73×10^2	1.12×10^5
11	1963	3.50	185.4	650	150	550	3.50×10^2	1.44×10^5
12	2043	3.80	189.0	720	100	430	1.92×10^2	7.88×10^4
13	2040	3.80	187.2	710	100	520	1.89×10^2	7.75×10^4
14	2058	3.80	188.0	715	100	530	1.70×10^2	6.97×10^4
15	2090	3.85	188.3	725	60	590	1.58×10^2	6.58×10^4
16	2105	3.85	188.4	726	60	380	1.67×10^2	6.82×10^4

Table A-2. Beryllia radiant heater data for 31-h run

Run no.[a]	Temperature, °F	Sheath voltage, V	Sheath current, mA	Ceramic resistance, ohm	Resistivity, ohm-cm	$\frac{Log_{10}R_m}{Log_{10}R_{in.}}$	Time, h
1	2000	150	190	790	3.24×10^5	0.970	4.0
2	1990	150	175	857	3.51	0.970	4.5
3	1990	150	155	968	3.97	0.979	5.5
4	2120	150	205	732	3.00	1.039	6.0
5	2110	150	230	653	2.68	1.024	6.5
6	2100	150	232	646	2.65	1.014	7.0
7	2060	150	218	688	2.82	0.994	7.5
8	2030	150	120	1250	5.13	1.023	10.0
9	2010	150	50	3000	12.30	1.077	12.5
10	2010	150	270	555	2.28	0.949	13.0
11	2080	150	185	540	2.21	0.987	13.8
12	2110	150	180	555	2.28	1.011	14.0
13	2110	150	155	967	3.96	1.056	14.5
14	2110	150	130	1150	4.72	1.069	15.5
15	2170	150	80	1870	7.67	1.152	15.5
16	2260	150	370	405	1.66	1.089	15.75
17	2110	150	50	3000	12.30	1.149	17.5
18	2105	150	50	3000	12.30	1.144	17.7
19	2090	150	45	3330	13.65	1.139	18.3
20	2070	150	35	4280	17.55	1.144	19.3
21	2075	150	35	4280	17.55	1.149	20.3
22	2040	150	70	2160	8.86	1.074	20.8
23	2220	150	100	1500	6.15	1.176	21.5
24	2160	150	65	2310	9.47	1.165	21.75
25	2190	150	90	1668	6.84	1.161	22.75
26	2165	150	70	2140	8.77	1.162	23.75
27	2205	150	120	1250	5.13	1.147	25.5
28	2180	150	155	968	3.97	1.106	25.5
29	2025	150	80	1875	7.69	1.050	25.5
30	2260	150	235	638	2.62	1.129	25.75

[a]Runs correspond to consecutive points on Fig. 15.

Table A-2 (contd)

Run no.[a]	Temperature, °F	Sheath voltage, V	Sheath current, mA	Ceramic resistance, ohm	Resistivity, ohm-cm	$Log_{10}R_m$ $Log_{10}R_{in}$	Time, h
31	2250	150	225	666	2.73	1.128	26.0
32	2200	150	165	909	3.73	1.116	28.0
33	2090	150	120	1200	4.92	1.057	29.0
34	2110	150	7400	375	1.54	0.978	30.0
35	2100	25	300	83.3	0.342	0.848	30.0

Appendix B

Lithium Heater Stress Analysis

1. Thermal Stress Analysis of Heater

This component consists of a 1.275-ID $\times$ 0.125-wall Cb-1Zr tube containing 4 parallel tantalum-core heating elements. Each end of the heater proper is capped with a bulkhead through which the cluster of 4 heating elements passes. The assembly is 32 in. long (see Fig. B-1 for cross-sectional details). For this heater the working pressure is 300 psia.
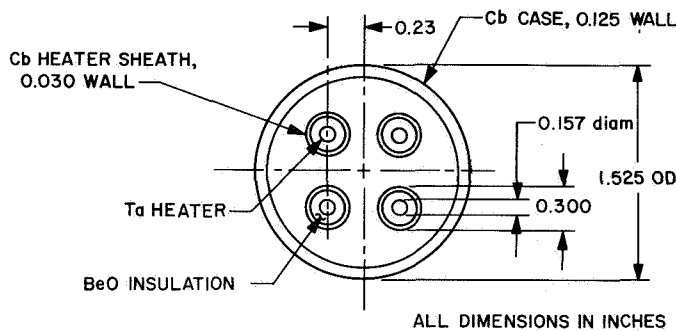

Fig. B-1. Section through heater

Equilibrium temperatures are

(1) Heating elements (including beryllium-oxide insulation and columbium alloy jacket) = 2200°F.

(2) Columbium alloy case = 2000°F.

The heater is assumed to be straight initially. Stress levels will be determined by calculating the forces required to return the several elements to the constrained length after having allowed them to expand individually without restraint. The fact that the effects of the shear gradient across the beryllium oxide insulation have been discounted will affect the results conservatively.

For stress calculation, the heating elements will be treated as a single member. Thus, a representative cross section would be as follows:
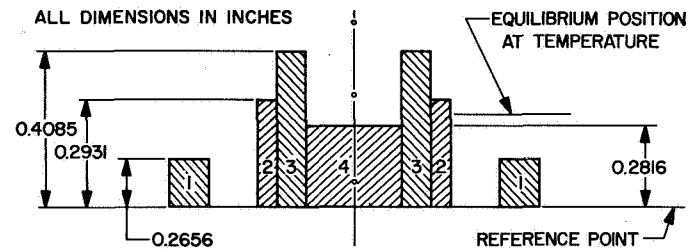
Data used in the calculations are tabulated below,

Item	Diagram item number	$E \times 10^{-6}$	Net area, in.^{2}	t, °F	$\alpha \times 10^6$ in./in. °F	Δl, in.
Cb case	1	13	0.55	1930	4.3	0.2656
Heater sheath	2	13	0.102	2130	4.3	0.2931
BeO insulation	3	10	0.1036	2130	6.0	0.4085
Ta rod	4	23	0.0774	2130	4.0	0.2816

where

α = coefficient of linear thermal expansion

Δl = thermal growth of member, $l\alpha\Delta t$

Δt = temperature change, °F

The equations which express the conditions existing when the members are forced to the equilibrium position are

(1) $P_1 + P_2 + P_3 + P_4 = 0$

where P = load in member due to restraint. (Subscripts correspond to numbers in diagram.)

(2) $\Delta l_1 + \dfrac{P_1 l_1}{A_1 E_1} = \Delta l_2 + \dfrac{P_2 l_2}{A_2 E_2}$

$$= \Delta l_3 + \dfrac{P_3 l_3}{A_3 E_3} = \Delta l_4 + \dfrac{P_4 l_4}{A_4 E_4}$$

where

Δl = thermal expansion

$\dfrac{Pl}{AE}$ = strain brought on by geometrical constraint

From these expressions, the P values are

$$P_1 = \quad 4{,}230 \text{ lb}$$

$$P_2 = \quad -350 \text{ lb}$$

$$P_3 = -4{,}010 \text{ lb}$$

$$P_4 = \quad 130 \text{ lb}$$

The unit stresses resulting from these loadings are

$$\sigma_1 = \frac{P_1}{A_1} = 7700 \text{ psi (tension; design limiting)}$$

$$\sigma_2 = -3430 \text{ psi (compression)}$$

$$\sigma_3 = -38{,}600 \text{ psi (compression)}$$

$$\sigma_4 = 1680 \text{ psi (tension)}$$

10,000-h rupture stress for Cb-1Zr at 2000°F = 3800 psi

From this consideration alone, it is recommended that the heater not be straight, but curved.

II. Hoop Stress

The results are aggravated only slightly by the effects of the 300-psi internal pressure and will not be dealt with in detail.

Hoop tension due to this pressure = pr/t

where

p = internal pressure, psi

r = ID/2, in.

t = wall thickness, in.

$$= \frac{300 \text{ psi} \,(0.6375 \text{ in.})}{0.125 \text{ in.}}$$

$$= 1530 \text{ psi (not design limiting)}$$

III. Bending Considerations of Heater

The development of the area moment of inertia I_x will be undertaken, neglecting the contribution of the tantalum rods.

$$I_{centroidal} \text{ of Cb case} = \frac{\pi}{64}(d_0^4 - d_i^4)$$

$$= 0.0491\,[(1.525)^4 - (1.275)^4]$$

$$= 0.1358 \text{ in.}^4$$

where d_0 and d_i are the outer and inner diameters. Similarly

$$I_{centroidal} \text{ of columbium heater sheaths} = 0.0491\,(d_0^4 - d_i^4)$$

$$= 0.0491\,(0.0081 - 0.0033)$$

$$= 0.000236 \text{ in.}^4$$

Transferred to the neutral axis of the composite beam

$$I_x = I_c + Ad^2$$

$$= 0.000236 + 0.7854\,[(0.300)^2 - (0.240)^2]\,(0.23)^2$$

$$= 0.00159$$

where A is the net area of member, and d is the distance from centroid to selected axis.

Four such sheaths represent $4\,(0.0159) = 0.00637$ in.^{4} The total I_x then is equal to $0.1358 + 0.00637 = 0.1422$ in.^{4} If

extreme fiber stress due to bending is limited to 3800 psi, then the maximum allowable bending moment is

$$M_{max} = \frac{\sigma I}{c}$$

where

σ = extreme fiber stress

I = section moment of inertia

c = distance from neutral axis to extreme fiber

$$= \frac{3800 \, \text{psi} \, (0.1422 \, \text{in.}^4)}{0.7625 \, \text{in.}}$$

$$= 710 \, \text{in.-lb}$$

This virtually rules out any possibility of bending difficulties arising from the dead weight of the charged heater if it is reasonably supported, since the charged heater weighs less than 15 lbs.

IV. Degree of Bending

The degree of bend required to relieve column loading on heater elements can be calculated from the geometry below:
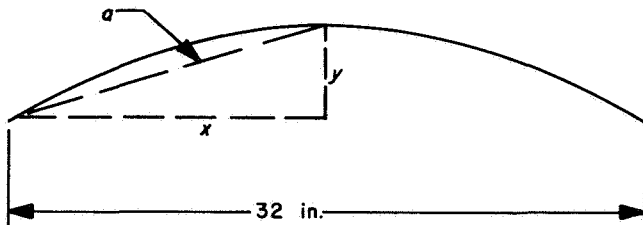
$$x^2 + y^2 = a^2, \qquad 2x + 2y \frac{dy}{dx} = 0,$$

$$\frac{dy}{dx} = -\frac{x}{y} \qquad \text{or} \qquad dy = -\frac{x}{y} dx$$

At operating temperature, the heater elements will be restrained from achieving their free expansion lengths by 0.0164 in. This is equivalent to 0.0082 at each end.

Lateral deflection of elements because of this axial compression when y is arbitrarily selected as 3 in. is

$$dy = -\frac{16}{3}(0.0082) = 0.0438 \, \text{in.}$$

End thrust required for this deflection is

$$\delta = e\left(\sec\frac{kl}{2} - 1\right)$$

where

$$k = (P/EI)^{1/2}$$

$$= e\left(\sec\frac{l}{2}(P/EI)^{1/2} - 1\right)$$

where

δ = lateral displacement of column, 0.0438 in.

e = loading eccentricity, 3 in.

l = column length, 32 in.

P = applied column loading, lb

E = Young's modulus of column material, psi

I = area moment of column section, in.^{4}

$I_{centroidal}$ for individual heater element:

$$\text{Columbium sheath} = \frac{\pi}{64}(d_0^4 - d_i^4)$$

$$= 0.0491\,[(0.300)^4 - (0.24)^4]$$

$$= 0.000236 \, \text{in.}^4$$

The tantalum rod will be considered an ellipse to convert it to equivalent columbium part. The diameter of the tantalum rod will be increased by the factor $E_{Ta}/E_{Cb} = 23/13 - 1.77$.

The 0.157-diam rod thus becomes an ellipse 0.157 × 0.278

$$I \text{ for this ellipse} = \pi a^3 b/4$$

where

a = semimajor axis, 0.139 in.

b = semiminor axis, 0.078 in.

Thus,

$$I = 0.7854\,(0.139)^3\,(0.078)\ \text{in.}^4 = 0.000165$$

Total I = 0.0004 in.^{4} (beryllium oxide neglected)

Solving for P in the column equation,

$$P = \frac{4EI}{l^2}\left(\cos^{-1}\frac{e}{\delta + e}\right)^2$$

$$= \frac{4\,(13 \times 10^6\,\text{psi})\,(0.0004\,\text{in.}^4)\,(\cos^{-1}0.98561)}{32^2} = 0.59\,\text{lb}$$

This result, for each of the four heating elements, is the axial loading that each must receive to adjust to the thermally induced dimensional inconsistency. Obviously no structural damage can occur from this light loading.

The eccentricity arbitrarily selected as 3 in. can be achieved by a 42-in. radius of curvature.

Nomenclature

d_c, d_1 center-conductor diameter, ft

d_i outer diameter of insulation, ft

d_t, d_0 outer diameter of sheath, ft

d_2 bus diameter, ft

E maximum allowable ceramic gradient, V/ft

I current in conductor, A

k_1 thermal conductivity of center conductor, Btu/h ft °F

k_i average thermal conductivity of insulator Btu/h ft °F

k_t average thermal conductivity of sheath, Btu/h ft °F

L_1 length of exposed center conductor, ft

L_2 minimum bus length, ft

N total number of heaters

n number of heaters in a series connection ($n = 1$ if all heaters are in parallel)

P_e electrical power output, kW

q''' volumetric heat release in bus, Btu/h ft³

T_b temperature of bus at point of heater attachment, °R

T_c temperature of center conductor, °R

V power supply voltage, V

Δt_i minimum allowable insulator thickness, ft

ε emissivity of bus

η_f radiation or fin efficiency of bus

θ_c temperature difference from center conductor to sheath surface, °F

ρ resistivity of center conductor, ohm-cm

σ Stefan-Boltzmann constant, 0.1714×10^{-8} Btu/h ft² °R⁴

References

1. Elliott, D. G., Cerini, D. J., Hays, L. G., and Weinberg, E. "Theoretical and Experimental Investigation of Liquid Metal MHD Power Generation," in *Electricity from MHD, Vol. II*, Document SM-74/177, *Third Symposium on Magnetohydrodynamic Electrical Power Generator*, Salzburg, 1966, pp. 995–1018. (Published by IAEA, Vienna, 1966.)

2. Kelly, R. J., *Lithium Corrosion Investigation of a High Power Columbium Alloy System*, Report PWAC-381, United Aircraft Corp., Pratt & Whitney Aircraft Div., (CANEL), Middleton, Connecticut, Feb. 1963.

3. Nichols, L. R., et al., *Design and Operational Performance of a 150-kilowatt Sodium Flash Vaporization Facility*, NASA TN D-1661. National Aeronautics and Space Administration, Washington, D. C., May 1963.

4. Hoffman, E., and Holowach, J., *New Components for Refractory Metal–Alkali Metal Corrosion Test Systems*, AEC Conf. 650411, TID 4500. AEC-NASA Liquid Metals Information Meeting, Gatlinburg, Tenn., April 21-23, 1965, pp. 149–214.

References (contd)

5. Tippets, F. E., and Converse, G. L., *Alkali Metals Boiling and Condensing Investigations,* Quarterly Progress Report No. 9, June 30–September 30, 1964, NASA-CR-54215. General Electric Co., Missile and Space Div., Cincinnati, Ohio.

6. Noyes, R. C., *Boiling Studies for Sodium Reactor Safety. Part I: Experimental Apparatus and Results of Initial Tests and Analysis,* NASA-SR-7909. North American Aviation, Inc., Atomics International Div., Canoga Park, Calif., Aug. 30, 1963.

7. Hays, L., *Investigation of Condensers Applicable to Space Power Systems,* Report EPS 1588-F. Electro-Optical Systems, Inc., Pasadena, Calif., Nov. 1962.

8. Fraas, A., et al., *Medium Power Reactor Experiment,* ORNL-3748. Oak Ridge (Tenn.) National Laboratory, Sept. 1964.

9. Goldsmith, A., Waterman, T., and Hirschhorn, H., *Handbook on Thermophysical Properties of Solid Materials,* The Macmillan Co., New York, 1960.

10. Dwyer, O., "Eddy Transport in Liquid Metal Heat Transfer," *A.I.Ch.E. J.* Vol. 9, No. 2, pp. 261–268, Mar. 1963.

11. Mackay, D., and Bacha, C., *Space Radiator Analysis and Design,* ASD-TDR-61-30. Wright-Patterson Air Force Base, Aeronautical Systems Div., Ohio, Oct. 1961.

12. Davis, J. P., Kikin, G. M., and Wolfson, L. S., *Lithium-Boiling Potassium Refractory Metal Loop Facility,* Technical Report 32-508, Jet Propulsion Laboratory, Pasadena, Calif., Aug. 1963.

13. Bacon, J., *The Evaluation of Materials for the Application to Magnetohydrodynamic Power Generation,* A-210173-1. United Aircraft Corp., Pratt & Whitney Aircraft Div., East Hartford, Conn., 1962.

14. Ryshkewitch, E., *Oxide Ceramics,* Academic Press, New York, 1960.

15. Knoll, M., *Materials and Processes of Electron Devices.* Springer-Verlag, Berlin, 1959.